

# CHAPTER 3

## MW-PECVD REACTOR DESIGN

In this chapter, our MW-PECVD design will be presented. The first section of this chapter describes the vacuum chamber design. Next, the microwave guiding components including rectangular waveguide, mode excitation design and cylindrical cavity design will be presented. In this section, we will describe the cutoff frequency and mode pattern ( $TE_{10}$  mode), followed by cylindrical cavity design. We will also describe the ideal of coupling mode and the resonant cavity used for our MW-PECVD reactor. In the last section, the set up of gas-flowing system will be presented.

### 3.1 Vacuum Chamber Design

The main body of vacuum chamber is constructed from stainless steel cylinder with outer diameter of 219 mm and height of 254 mm. The vacuum chamber has six ports connected to the bottom plate, the front plate, the left plate, the right plate (ISO 63), the rear plate (ISO 63), and the top plate, as showed in Fig. A.1. The photograph of system is showed in Fig. 3.1 and the details each of flanges are described clearly in appendix A.1.

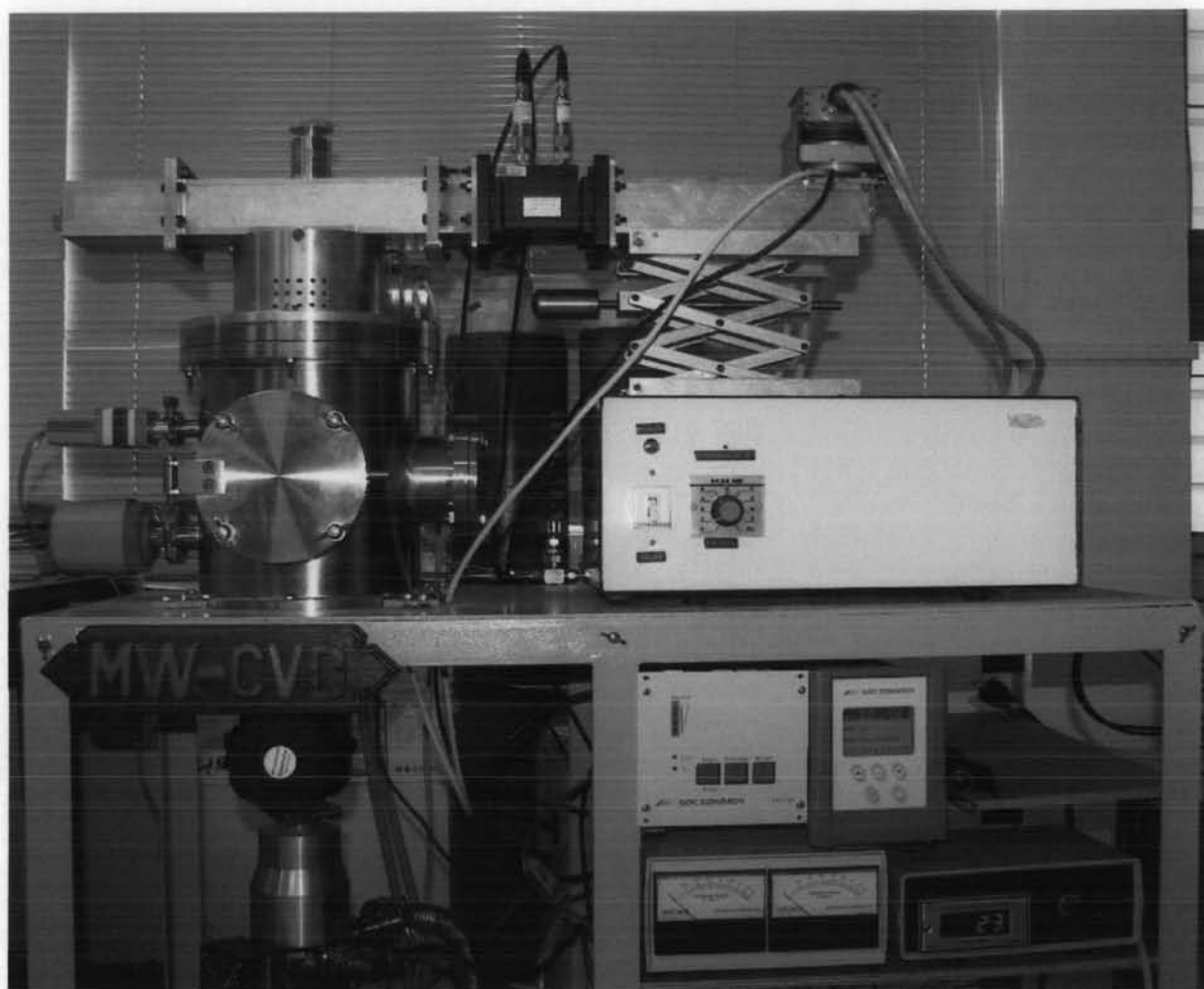


Figure 3.1: The photograph of MW-PECVD reactor.

## 3.2 Microwave Guiding Components

### 3.2.1 Rectangular waveguide and mode excitation design

Microwave is an electromagnetic waves with wavelengths in the range of 1-cm to 1-m or corresponding frequency in the range 300 MHz to 30 GHz [39]. Traditional microwave plasma research, mostly utilize at 2450 MHz (2.45 GHz) which is the same as in ordinary microwave oven. The common transmission line in this frequency is a hollow-pipe waveguide. The dimensions of waveguide depend on the specified frequency range of which its electromagnetic wave can propagate and relate to the cutoff frequency ( $f_{c_{mn}}$ ). The lowest frequency of an electromagnetic wave that can propagate is called cutoff frequency. In rectangular and circular waveguide, the propagation waves can be in both  $TE_{mn}$  modes (transverse electric, no electric field component in the direction of propagation) and the  $TM_{mn}$  modes (transverse magnetic, no magnetic field in the direction of propagation) which m and n are the integers followed from Helmholtz equation. The calculation details of cutoff frequency for rectangular and circular waveguide are presented in appendix B.1.1 and B.1.2, respectively.

In this study, the microwave energy source (magnetron head) is supplied by MUEGGE ELECTRONIC GmbH. The photograph of magnetron head is showed in Fig. 3.4 of which the specification is given in appendix D.1.1.

### 3.2.2 Magnetron power supply

Fig. 3.2 shows the schematic diagram of microwave power source. In the circuit diagram, it consists of two main parts, which are low and high voltage circuits. For the low voltage circuit, the transformer (4.5VAC, 15A) supplies current to the magnetron filament.

The full-circle double rectify is used for the high voltage circuit. Two series of high voltage diode (Sr101) connected as forward and reverse bias are parallely

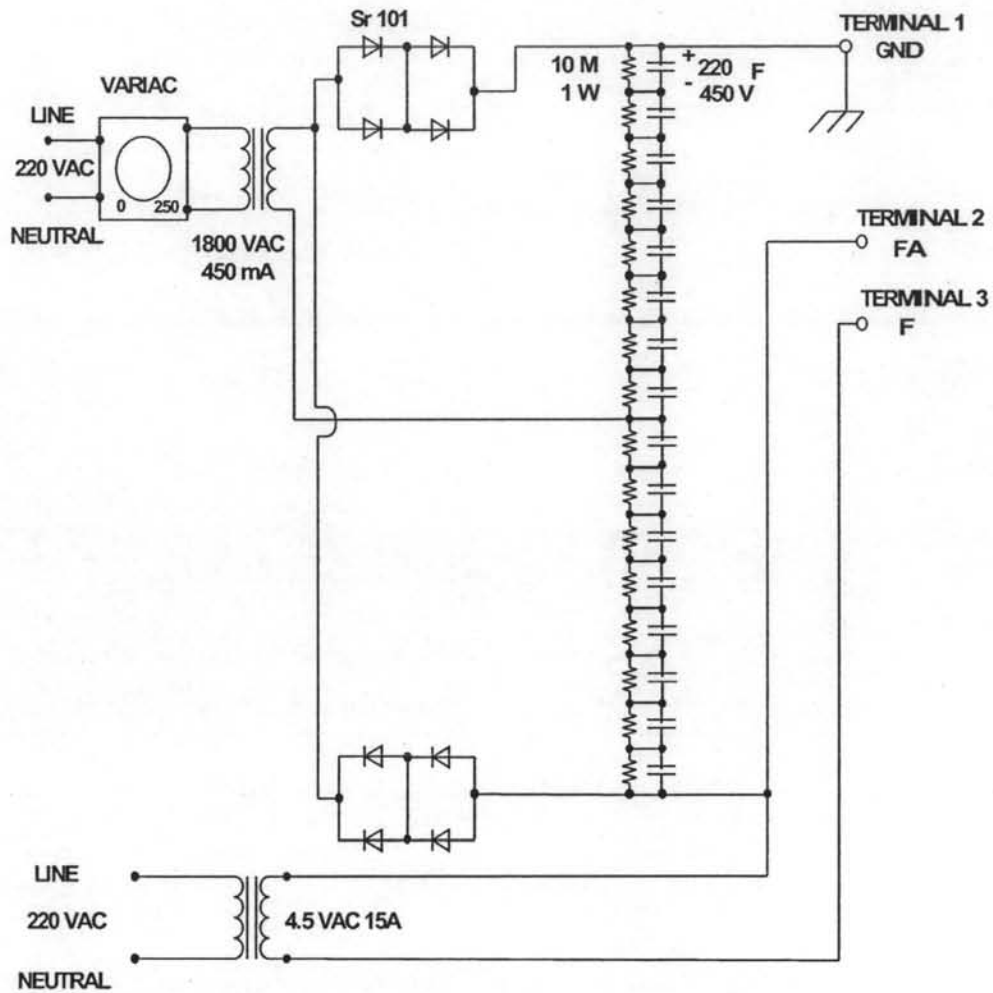


Figure 3.2: Circuit diagram supplied to magnetron head

connected with the series of high voltage capacitor ( $220\mu\text{F}$ ,  $450\text{V}$ ) in order to rectify the full wave. The series of resistors ( $10\text{M}\Omega$ ,  $1\text{W}$ ) are parallelly connected with the high voltage capacitor to safety discharge in the case of load misplaced. In should be noted that the magnetron head is the load for the source. The output voltage is controlled by adjusting the variac via transformer ( $1800\text{VAC}$ ,  $450\text{mA}$ ), which can generate the voltage to approximately  $4500\text{ V}$ , as illustrated in Fig. 3.3, which is the threshold voltage for the magnetron to release the microwave.

An air-filled aluminium rectangular waveguide based on WR340 standard ( $86.4\times 43.2\text{ mm}^2$ ) is designed. Due to this dimensions, only the  $\text{TE}_{10}$  mode can

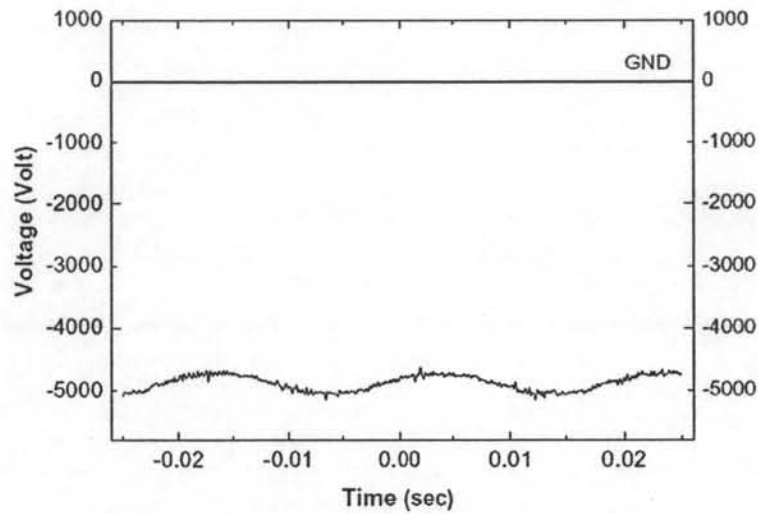


Figure 3.3: Signal of high volt supplied to magnetron head

propagate. Furthermore, the high conductivity of aluminium ( $3.816 \times 10^7$  S/m [40]) is a cause for low skin depth for microwave. As already mentioned that its dimensions is related to the cutoff frequency which is showed in equation B.11 in appendix B. For the WR340, the cutoff frequency is 1.72 GHz (inside width (a)=86.4mm, and inside height (b)=43.2mm) which is less than 2.45 GHz, so the electromagnetic wave can propagate.

Furthermore, the wavelength within waveguide ( $\lambda_g$ ) also relates to the free space wavelength ( $\lambda_0 = 121.6$  mm), by the relation [41];

$$\lambda_g = \frac{\lambda_0}{\sqrt{1 - (f_c/f)^2}}. \quad (3.1)$$

For  $f_c$  of 1.72 GHz and  $f$  of 2.45 GHz, the value of  $\lambda_g$  become 170 mm. Rectangular waveguide is designed with the length of 679.5 mm, as showed in Fig. 3.5. However, we can adjust the adjustable plunger to match the seventh node of  $\lambda_g/2$  to generate a standing wave. The magnetron head is coupled via this waveguide at distance of 22 mm from end cap (see Fig. 3.5), which is used as a standard coupling [41]. The microwave power is measured by GAE dual power

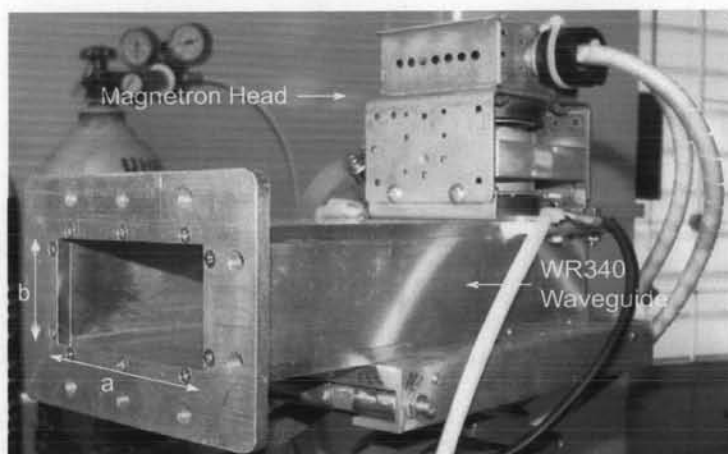


Figure 3.4: The photograph of 2M137W/J magnetron head and WR340 an air-filled aluminium rectangular waveguide.

monitor model GA3007 (no.19 in Fig. A.4).

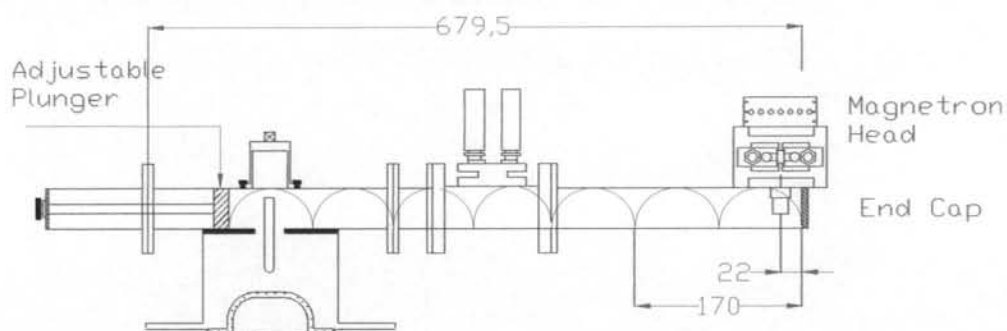


Figure 3.5: The schematic diagram of the waveguide from our design in millimeter unit. The dotted lines indicate the amplitude variation of the electric field.

Assuming propagation in the  $+Z$  direction, for  $TE_{10}$  mode which is the mode in our rectangular waveguide design, the electric and magnetic field components [39] are described by the following;

$$H_z = A \cos \frac{\pi x}{a} e^{-ik_g z}, \quad (3.2)$$

$$H_x = i \frac{k_g}{k_c} A \sin \frac{\pi x}{a} e^{-ik_g z}, \quad (3.3)$$

$$E_y = -iAZ_h \frac{k_g}{k_c} \sin \frac{\pi x}{a} e^{-ik_g z}. \quad (3.4)$$

The parameters such as  $k_g$ ,  $k_c$ , and  $Z_h$  are the propagation factor, the cutoff wave number, and wave impedance, respectively. In order to excite the strong electric field of  $TE_{10}$  mode in rectangular waveguide, an antenna of magnetron head is placed vertically at  $x = a/2$  ( $a$  is a 86.4 mm).

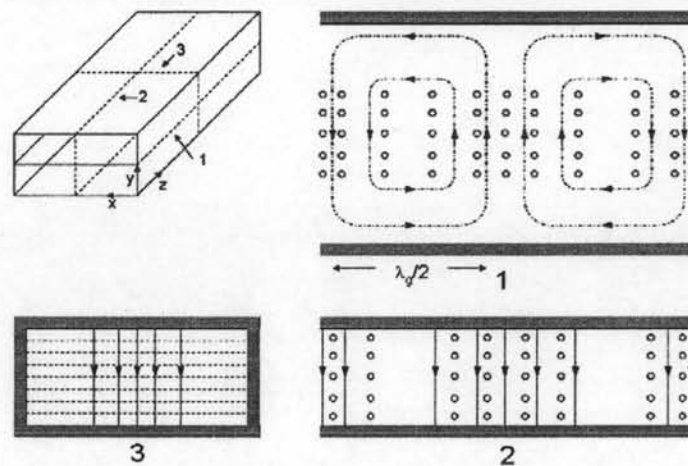


Figure 3.6: Electric and magnetic field lines for  $TE_{10}$  mode in rectangular waveguide [40].

### 3.2.3 Cylindrical cavity resonator design

The air-filled aluminium cylinder waveguide with 140 mm inside diameter and 82.5 mm height is designed as a cavity resonator, as showed in Fig. 3.7. According to the cutoff frequency of cylindrical waveguide as showed in equation 3.5, we can see that each mode of the cutoff frequency depends on the zero order of Bessel functions of the first kind (the values of  $\alpha_{mn}$  is illustrated in Table B.1) and the radius of the waveguide ( $a$ ).

$$f_{c_{mn}} = \left[ \frac{c}{2\pi} \right] \left[ \frac{\alpha_{mn}}{a} \right]. \quad (3.5)$$



In our design, the radius of cylindrical waveguide is a 70 mm, which corresponds to the  $TM_{10}$  mode propagation. The calculation of cutoff frequency in  $TM_{01}$ ,  $TM_{11}$ , and  $TM_{21}$  with this 70 mm radius is showed in Table 3.1. We can see that only the wave in  $TM_{01}$  mode can propagate.

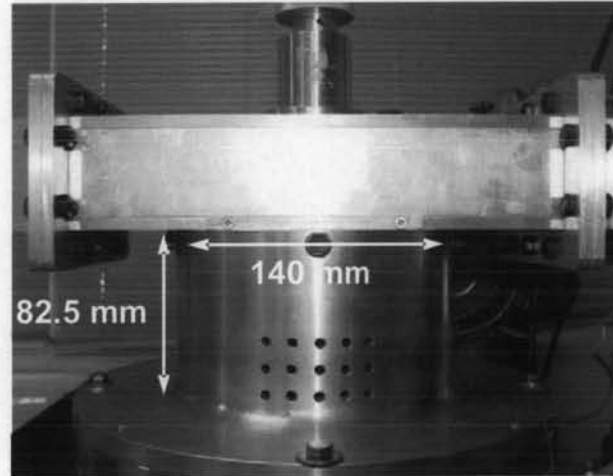


Figure 3.7: The photograph of cylindrical resonator.

Table 3.1: The values of cutoff frequency in  $TM_{01}$ ,  $TM_{11}$ , and  $TM_{21}$  modes with the radius of circular waveguide.

Radius (mm)	$f_{c,01}$ (GHz)	$f_{c,11}$ (GHz)	$f_{c,21}$ (GHz)
70.0	<b>1.64</b>	2.61	3.50
74.0	<b>1.55</b>	2.47	3.31
75.0	<b>1.53</b>	<b>2.44</b>	3.27
80.0	<b>1.44</b>	<b>2.29</b>	3.07
90.0	<b>1.28</b>	<b>2.03</b>	2.72

The perforated cylinder side wall allows the observation of plasma inside the bell jar underneath as well as allowed the forced-air cooling to flow through. The top of cylinder cavity is connected with WR340 waveguide which has an open for the adjustable brass antenna to feed into the resonant (see Fig. 3.5).



According to the  $TE_{10}$  mode pattern in rectangular waveguide as showed in Fig. 3.6, the adjustable brass antenna must be located at the strong electric field. Therefore, in our design, the antenna is located at a quarter  $\lambda_g$  from the shorted end of adjustable plunger where the electric field intensity is maximum [41, 42, 43]. However, the dimension of designed brass antenna, we do not clear for it.

When the electromagnetic wave is generated from magnetron head, wave in  $TE_{10}$  mode in rectangular waveguide is converted to  $TM_{01}$  mode (the mode pattern of  $TM_{01}$  is showed in Fig. 3.8) into cylinder waveguide via this antenna.

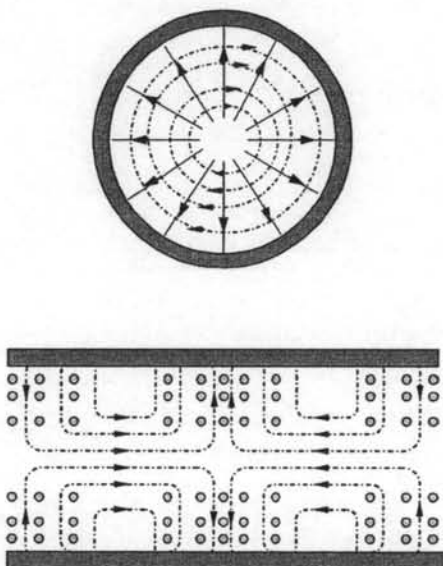


Figure 3.8: Electric and Magnetic field lines for  $TM_{01}$  mode in circular waveguide [40].

Furthermore, the close plates at each of circular waveguide in our design, the resonant frequency of  $TM_{mn}$  modes in cylindroid can be expressed by equation 3.6 [40]

$$f_{mnl} = \frac{c}{2\pi} \sqrt{\left(\frac{\alpha_{mn}}{a}\right)^2 + \left(\frac{l\pi}{d}\right)^2}, \quad (3.6)$$

where  $\alpha_{mn}$ ,  $a$ , and  $d$  are the zero of Bessel functions of the first kind, the radius and the height of circular waveguide, respectively. The cylindrical cavity has the

radius of 70 mm, and height of 82.5 mm to correspond with  $TM_{011}$  mode at 2.45 GHz resonant frequency.

It should be noted that the electric field lines must be perpendicular to the surface of waveguide while the magnetic field lines from a closed loop is parallel with the waveguide and perpendicular to the electric field.

### 3.3 Gas-Flowing System

The gas-flowing system consists of the hydrogen ( $H_2$ ) and methane ( $CH_4$ ) tanks, regulators and mass flow controllers (MFCs). MESSER regulators are used to reduce pressure from 10 bar ultra high purity (99.999%)  $H_2$  and  $CH_4$  tanks. Gases are regulated by MFCs to obtain accurate gas-flow rates. Each of gases flows into a manual on-off valves. Then, gases are mixed at gas mixing line. Gases flow to manual on-off valves again before flow into the reactor chamber. The schematic diagram of gas-flowing is showed in Fig. 3.9. In this work, the flow of  $H_2$  is controlled by Aalborg model GFC-17 and  $CH_4$  gas is controlled by Dwyer model GFC-2102.

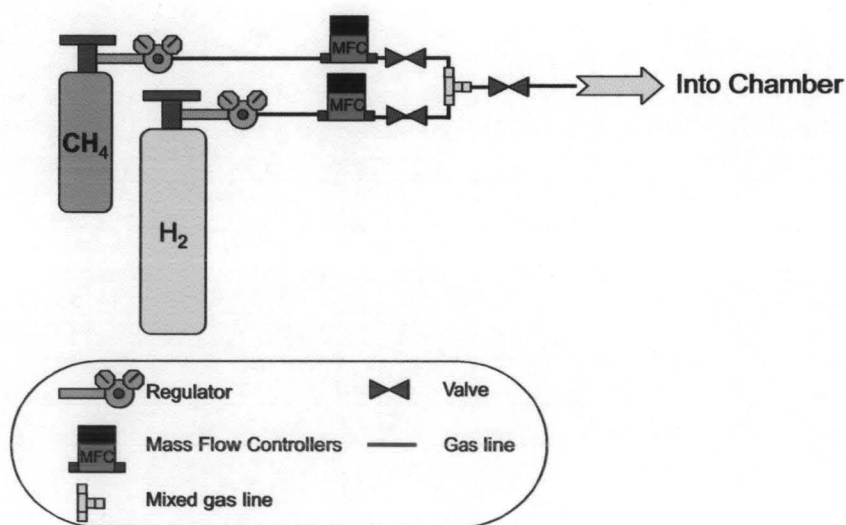


Figure 3.9: Schematic diagram of gas-flow system.

It should be noted that due to the MFCs manufacturer calibration to a specific reference gas, a relative K factor is required for the adjustment of each actual experiment gas. For example, if we want to know the flow rate of methane and wish to calibrate with nitrogen at 1.39 sccm, the actual flow rate of methane is;

$$Q_{CH_4} = Q_r \times K = 1.39 \times 0.7175 = 1.00 \text{ sccm} , \quad (3.7)$$

where  $Q_r$  is mass flow rate of the reference gas, which is showed on the MFCs display, and K is relative K factor to reference gas (methane to nitrogen).

### 3.4 Plasma Temperature

We have used the optical emission spectroscopy (OES) technique with the Boltzmann plot method to determine the electron excitation temperature ( $T_{exc}$ ) in our MW-PECVD reactor. The  $T_{exc}$  can be obtained using the equation 3.8 [44],

$$\ln [I_{em}^{nm} \lambda_{nm} / g_n A_{nm}] = C - E_n / k T_{exc}, \quad (3.8)$$

where  $I_{em}^{nm}$ ,  $\lambda_{nm}$ , and  $A_{nm}$  are the line intensity of the emitting light, wavelength, and the transition probability from level n to m, respectively.  $E_n$  and  $g_n$  are the upper energy level and statistical weight, respectively.  $C$  is constant, and  $k$  is the Boltzmann constant. It should be noted that the spectroscopic data of Ar were obtained from NIST Atomic Spectra Database [45].

In this work, the ocean optic type HR4000 including OOIBase 32 software program was used to collect the emitting light from argon (Ar) plasma. The fiber optics was situated at out side of perforate cylinder wall, approximate distance of 26 mm from the quartz bell jar. Fig. 3.10 shows the optical emission spectra of Ar plasma. It exhibits the most spectrum lines of ArI in the range of 720 to 950 nm.

Table 3.2 lists the spectroscopic data needed for the twelve argon transition used in this work.

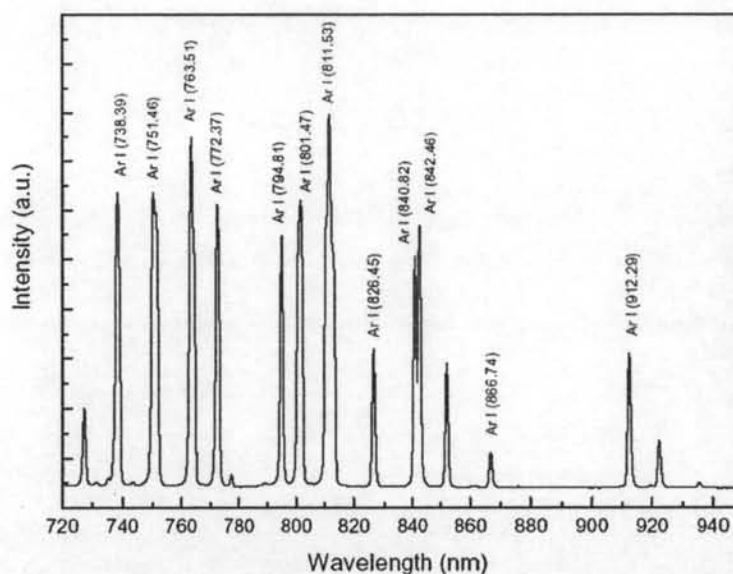


Figure 3.10: Optical emission spectrum of Ar plasma in the range of 720 to 950 nm. The labeled emission lines are ArI.

From equation 3.8, we can plot the natural log of  $I_{em}^{nm} \lambda_{nm} / g_n A_{nm}$  against the energy of excited state. The inverse of slope is  $T_{exc}$  in electron volt unit. An example of Boltzmann plot is presented in Fig. 3.11.

The observation of  $T_{exc}$  as a function of pressure is showed in Fig. 3.12. We found that the  $T_{exc}$  of Ar plasma in our MW-PECVD reactor was varied from 0.82 to 1.06 eV over the pressure of 0.15 to 7.0 Torr at microwave power of 300 watts.

Table 3.2: ArI spectroscopic data.

Wavelength (nm)	$E_n$ (eV)	$g_n$	$A_{nm}(s^{-1})$
738.39	13.30	5	8470000
751.46	13.27	1	40200000
763.51	13.17	5	24500000
772.37	13.15	3	51800000
794.81	13.28	3	18600000
801.47	13.09	5	9280000
811.53	13.07	7	33100000
826.45	13.32	3	15300000
840.82	13.30	5	22300000
842.46	13.09	5	21500000
866.79	11.72	1	2430000
912.29	12.90	3	18900000

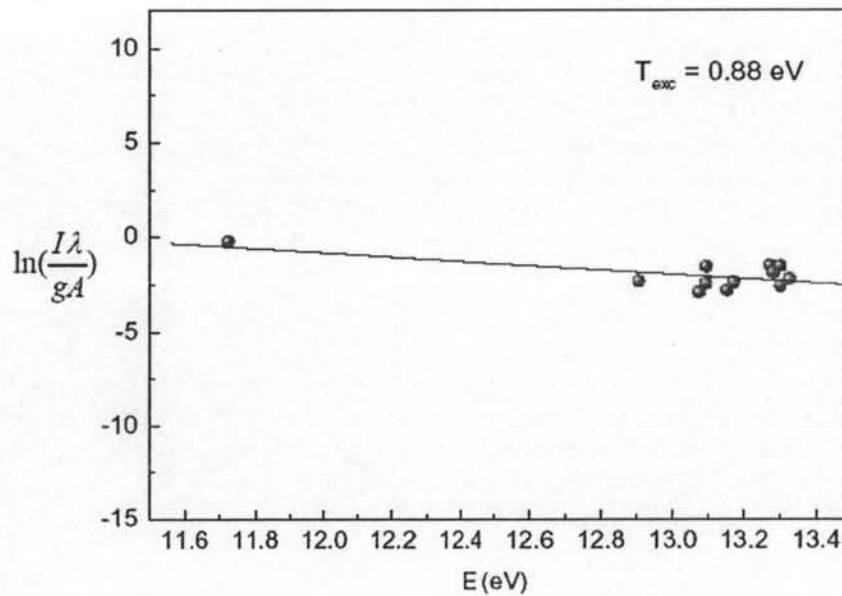


Figure 3.11: Typical Boltzmann plot obtained by ArI lines of the plasma.

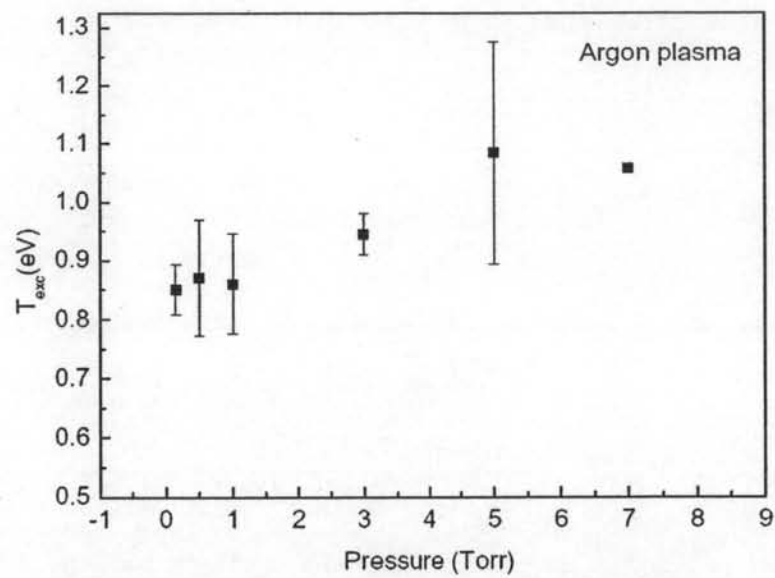


Figure 3.12:  $T_{exc}$  against pressure at microwave power of 300 watts.